Acta Crystallographica Section D
Biological Crystallography
ISSN 0907-4449

Structures of human oxy- and deoxyhaemoglobin at different levels of humidity: variability in the T state

B. K. Biswal and M. Vijayan*

Molecular Biophysics Unit, Indian Institute of Science, Bangalore 560 012, India

Correspondence e-mail: mv@mbu.iisc.ernet.in

Received 5 December 2001
Accepted 18 April 2002

PDB References: oxyhaemoglobin, 93% r.h., 1lfq, r1lfqsf; oxyhaemoglobin, 90% r.h., 1lft, r1lftsf; oxyhaemoglobin, 88% r.h., 1lfv, r1lfvsf; oxyhaemoglobin, 84% r.h., 1lfy, r1lfysf; oxyhaemoglobin, 25% methanol, 1lfz, r1lfzsf; deoxyhaemoglobin, 90% r.h., 1lfl, r1lflsf.

High-salt crystals of human oxy- and deoxyhaemoglobin have been studied at different levels of environmental humidity and solvent content. The structure of the oxy form remains relatively unchanged at all levels. The deoxy form, however, undergoes a water-mediated transformation when the relative humidity around the crystals is reduced below 93%. The space group is maintained during the transformation, but the unit-cell volume nearly doubles, with two tetrameric molecules in the asymmetric unit of the low-humidity form compared with one in the native crystals. Interestingly, the haem geometry in the low-humidity form is closer to that in the oxy form than to that in the native deoxy form. The quaternary structure of one of the tetramers moves slightly towards that in the oxy form, while that in the other is more different from the oxy form than that in the high-salt native deoxy form. Thus, it would appear that, as in the case of the liganded form, the deoxy form of haemoglobin can also access an ensemble of related T states.

1. Introduction

We have been exploring protein hydration and its consequences using an approach involving water-mediated transformations in which protein crystals undergo reversible transformations with a change in the water content when the environmental humidity is systematically varied (Salunke *et al.*, 1984, 1985; Kodandapani *et al.*, 1990; Madhusudan & Vijayan, 1991; Madhusudan *et al.*, 1993; Radha Kishan *et al.*, 1995; Nagendra *et al.*, 1995, 1996, 1998; Sadasivan *et al.*, 1998; Sukumar *et al.*, 1999; Biswal *et al.*, 2000). Using this approach, it has been possible to establish a relationship between hydration, mobility, accessibility and action in hen egg-white lysozyme and bovine pancreatic ribonuclease A (Kodandapani *et al.*, 1990; Radha Kishan *et al.*, 1995; Nagendra *et al.*, 1998; Sadasivan *et al.*, 1998; Biswal *et al.*, 2000). In particular, it was established that the overall changes in molecular geometry resulting from the transformation from the native to the low-humidity forms are similar to those that occur during enzyme action. It also turns out that such changes are more pronounced in the active-site region. In another interesting observation, the crystal structure of monoclinic lysozyme with extremely low solvent content (9.4%) suggested that the loss of activity that accompanies dehydration could be the result of the removal of functionally important water molecules from the active-site region and the reduction of the size of the substrate-binding cleft (Nagendra *et al.*, 1998).

The above results encouraged us to extend the studies involving water-mediated transformations to complex multimeric proteins. The obvious choice in this context was haemoglobin, the most thoroughly investigated multimeric protein. Haemoglobin is an $\alpha_2\beta_2$ tetrameric transport protein of molecular weight 64 500 Da. Much of the current understanding of the allosteric mechanism has resulted from studies on haemoglobin (Perutz *et al.*, 1998; Tame, 1999). In pursuance of the allosteric model proposed by Monod *et al.* (1965), haemoglobin exists in two states, a low-affinity state (T) and a high-affinity state (R). A stereochemical mechanism for the cooperative effects in the tetrameric protein was first proposed by Perutz (1970) primarily on the basis of horse deoxyhaemoglobin (Bolton & Perutz, 1970) and methaemoglobin (Perutz *et al.*, 1968). This mechanism is based on the equilibrium between the tense (T) deoxy state and the relaxed (R) liganded state. Subsequently, new relaxed states have been characterized (Silva *et al.*, 1992; Smith & Simmons, 1994; Kroeger & Kundrot, 1997; Mueser *et al.*, 2000, Biswal & Vijayan, 2001).

The equilibrium between R and T conformations is modulated by ions, such as H^+, CO_2, phosphates and Cl^-. Water has also been proposed to be an allosteric regulator (Colombo *et al.*, 1992). In particular, it has been suggested that the transition from the T to the R state is accompanied by the uptake by the protein of several dozen water molecules (Colombo *et al.*, 1992; Colombo & Seixas, 1999).

The effect of, among other things, change in humidity on the crystal packing of horse methaemoglobin was explored in the early days of protein crystallography (Boyes-Watson *et al.*, 1947; Huxley & Kendrew, 1953; Perutz, 1954) in order to derive phase information on some special reflections. Protein crystallography was then in its infancy and the work was not followed up by detailed structure analysis. In the meantime, attention shifted substantially from horse to human haemoglobin. Thus, in our study, we concentrated on human deoxy-, oxy- and methaemoglobin. While the crystal structures of human deoxyhaemoglobin (Fermi *et al.*, 1984) and oxyhaemoglobin (Shaanan, 1983) are known, the structure of human methaemoglobin has surprisingly not been determined. Therefore, the methaemoglobin structure, with three tetramers in the asymmetric unit, was analysed (Biswal & Vijayan, 2001). The structure demonstrated that the three molecules have quaternary structures intermediate between those of the R and the R2 structures. R2, observed in crystals grown from a low-salt (0.1 *M*) medium (Silva *et al.*, 1992), is a relaxed structure substantially different from the conventional liganded form R found in crystals grown from a high-salt (2.5 *M*) medium. The same intermediate nature was also observed in the disposition of residues in the 'switch' region of human methaemoglobin molecules. However, the methaemoglobin crystals did not survive even the slightest reduction in environmental humidity. The subsequent studies were therefore confined to human oxy- and deoxyhaemoglobin crystals. The results of these studies are reported here.

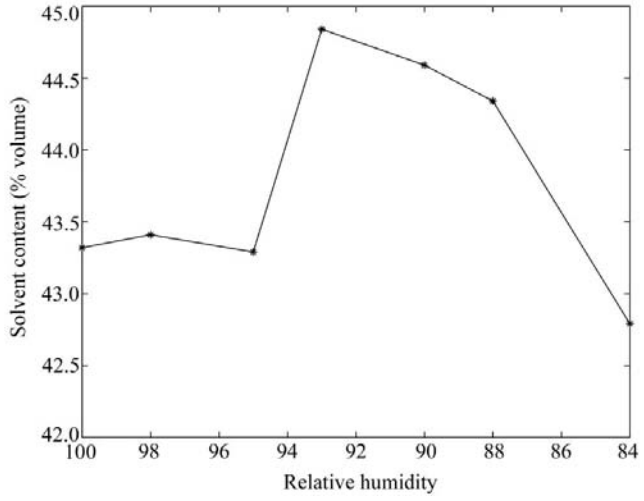

Figure 1
Variation in solvent content as a function of relative humidity in the crystals of oxyhaemoglobin.

2. Experimental

2.1. Sample preparation

Human haemoglobin was purified from fresh human blood and crystals of the oxy and deoxy forms were prepared using the protocol described by Perutz (1968). The crystallization buffer had a pH around 6.5 and a molarity of 2.5 *M*. Different low-humidity forms of the crystals were prepared by placing a drop of a supersturated solution of an appropriate salt ($CuSO_4.5H_2O$ for a relative humidity of 98%, $Na_2HPO_4.12H_2O$ for 95%, $Na_2SO_4.10H_2O$ for 93%, $ZnSO_4.7H_2O$ for 90%, K_2CrO_4 for 88% and KBr for 84%) at about 1 cm from the crystal in a thin-walled capillary. Nearly a day was required for equilibration. A partially dehydrated form of oxyhaemoglobin was also obtained by using a drop of 25% methanol (Boyes-Watson *et al.*, 1947) instead of the salt solution.

2.2. Data collection

Intensity data from the native and the low-humidity forms of the crystals and from the partially dehydrated form of oxyhaemoglobin obtained using 25% methanol were collected on a MAR image plate mounted on an RU-200 Rigaku X-ray generator with a copper anode. Crystal-to-detector distances of 150 mm and 100 mm were used for the oxy and deoxy crystals, respectively. The data were processed and scaled using *DENZO* and *SCALEPACK* (Otwinowski & Minor, 1997).

2.3. Structure solution and refinement

The structures of the low-humidity forms and the 25% methanol form were solved by molecular replacement using the program *AMoRe* (Navaza, 1994), with protein molecules from the structures of human deoxyhaemoglobin (Fermi *et al.*, 1984) and human oxyhaemoglobin (Shaanan, 1983; PDB code 1hho) as search models as appropriate. All the structures were refined in a similar manner using *CNS* (Brünger *et al.*,

1998) incorporating the cross-validated maximum-likelihood refinement target. 50 cycles of rigid-body refinement treating each subunit as a rigid body were carried out. The model was subjected to a 4000 K Cartesian slow-cooling protocol, using the maximum-likelihood function as the target for refinement. At this stage a map was calculated and manual rebuilding was carried out using *FRODO* (Jones, 1978) wherever necessary. The refinement continued using *CNS*. Once it converged, typically around an R value of 0.23, identification of water molecules began. This was performed in several stages with the help of $2F_o - F_c$ and $F_o - F_c$ maps. After every cycle of model building a few cycles of group B-factor and positional refinement were performed. Cycles of position refinement, correction of model using Fourier maps and the identification of water molecules continued until no significant density remained in the map. $R_{\rm free}$ values were closely monitored throughout the refinement. Haem groups were refined by applying restraints to bond distances and angles in order to maintain proper geometry (Kuriyan *et al.*, 1986). During most of the refinement cycles, NCS restraints were applied separately to the α- and β-subunits in each structure. The restraints were progressively removed and no NCS restraints were used in the final cycles.

Towards the end of the refinement an omit map was calculated (Vijayan, 1980). Such a map is formally independent of the input coordinates and provides an unbiased representation of the structure. The model was carefully checked against this map and the necessary corrections were made. The stereochemical acceptability of the structure was checked using *PROCHECK* (Laskowski *et al.*, 1993).

3. Results and discussion

3.1. Preliminary data

The behaviour of the unit-cell parameters and hence the solvent content (calculated using the Matthews method; Matthews, 1968) in response to the systematic reduction in environmental humidity was unexpected in the case of oxyhaemoglobin. To start with, the unit-cell volume remained constant; the cell then expanded and the solvent content increased with further reduction in relative humidity (r.h.), reaching a maximum at about 93% r.h. (Fig. 1). Subsequent reduction in r.h. led to a reduction in the unit-cell volume and solvent content. The resolution of the data also progressively deteriorated, reaching 3.3 Å at 84% r.h. Further reduction in environmental humidity resulted in loss of crystallinity. The behaviour of the crystals of deoxyhaemoglobin in response to reduction in environmental humidity was, however, along the expected lines. The solvent content fell slightly in a continuous fashion until the r.h. was lowered to 93% (Fig. 2). Between r.h. 93 and 90% the crystal underwent a transformation with an abrupt loss of solvent. The unit-cell volume almost doubled (Fig. 3) without change in the space group. Two symmetry-related molecules now became crystallographically independent. It may be recalled that it is just the reverse of what happened in the water-mediated transformation in monoclinic lysozyme (Salunke *et al.*, 1985; Madhusudan *et al.*, 1993). Native monoclinic lysozyme contained two crystallographically independent molecules which became equivalent in the low-humidity form after transformation, with a halving of the unit-cell volume.

Data collected at r.h. values of 93, 90, 88 and 84% and those collected in the 25% methanol environment were used for further work on oxyhaemoglobin crystals. Native data were also collected and the structure refined using the data, but unless otherwise stated the structural results obtained earlier by Shaanan (1983) were used in comparative studies, as these data had better resolution. Data from the native deoxy crystals and the transformed deoxy crystals (90% r.h.) were collected and used for refinement. However, the deoxy native structure obtained by Fermi *et al.* (1984) was used for comparisons in view of the better resolution of that structure. Data were not

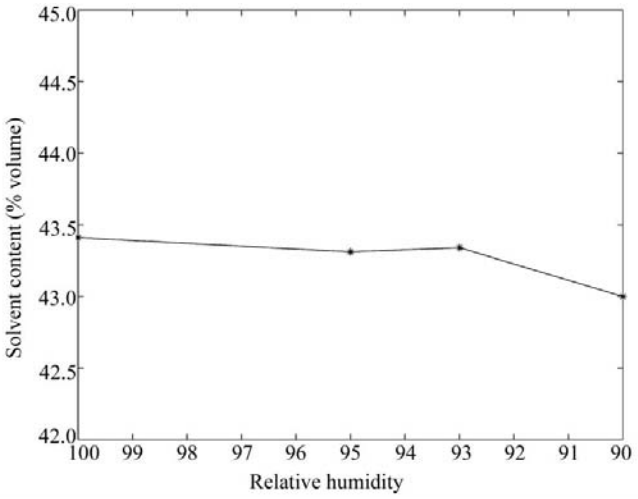

Figure 2
Variation in solvent content as a function of relative humidity in the crystals of deoxyhaemoglobin.

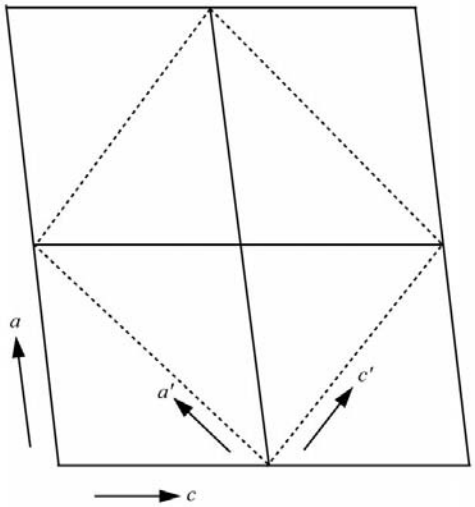

Figure 3
The relationship between the unit cells of the native and the low-humidity form of deoxyhaemoglobin. The primed symbols correspond to the low-humidity form.

Table 1
Crystal data and refinement statistics.

Values in parentheses refer to the highest resolution shell.

	Oxy	Oxy 93% r.h.	Oxy 90% r.h.	Oxy 88% r.h.	Oxy 84% r.h.	Oxy 25% methanol	Deoxy	Deoxy 90% r.h.
Space group	$P4_12_12$	$P4_12_12$	$P4_12_12$	$P4_12_12$	$P4_12_12$	$P4_12_12$	$P2_1$	$P2_1$
Unit-cell parameters (Å, °)	$a = b = 53.7$, $c = 193.8$	$a = b = 54.2$, $c = 195.7$	$a = b = 54.2$, $c = 194.9$	$a = b = 54.2$, $c = 194.2$	$a = b = 53.6$, $c = 193.3$	$a = b = 52.8$, $c = 192.1$	$a = 63.3$, $b = 83.3$, $c = 53.8$, $\beta = 99.4$	$a = 89.3$, $b = 82.9$, $c = 76.3$, $\beta = 99.3$
Unit-cell volume (Å^3)	558859.1	574896.2	572546.1	570489.7	555343.2	535544.1	279872.2	556435.7
Z	4	4	4	4	4	4	2	4
Solvent content (%)	43.3	44.8	44.6	44.3	42.8	40.6	43.4	43.0
Resolution range (Å)	20–2.5	20–2.6	20–2.6	20–2.8	20–3.3	20–3.1	20–2.1	30–2.7
Last resolution shell (Å)	2.6–2.5	2.7–2.6	2.7–2.6	2.9–2.8	3.4–3.3	3.2–3.1	2.17–2.1	2.8–2.7
No. of observations	66131	65312	50116	32801	16345	20857	145765	85616
No. of unique reflections	10041	9707	9245	7436	4467	5010	30095	30721
Completeness of data (%)	95.4 (92.8)	99.9 (100.0)	96.3 (99.4)	97.4 (99.3)	94.6 (95.4)	98.4 (98.2)	93.5 (93.2)	98.0 (99.4)
Merging R for all reflections (%)	12.1 (35.3)	12.9 (37.0)	12.8 (30.0)	11.7 (41.2)	10.4 (40.3)	11.4 (42.4)	11.0 (32.5)	11.5 (48.1)
Average $I/\sigma(I)$	5.4	5.8	7.9	8.0	4.1	4.2	7.6	6.4
R factor (%)	20.3	19.7	20.1	21.0	20.8	20.0	20.1	19.0
R_{free}	25.6	25.8	26.5	27.0	26.1	26.8	25.2	26.3
No. of protein atoms	2192	2192	2192	2192	2192	2192	4384	8768
No. of water O atoms	58	45	32	24	15	29	180	170
No. of haem atoms	86	86	86	86	86	86	172	344
R.m.s. deviation from ideality								
Bond distances (Å)	0.003	0.011	0.009	0.008	0.012	0.009	0.008	0.021
Bond angles (°)	1.4	1.3	1.2	1.3	1.4	1.4	1.2	1.2
Dihedral angles (°)	19.3	20.2	19.5	20.6	19.7	19.2	19.1	19.2
Improper angles (°)	1.3	1.5	1.2	1.3	1.4	1.5	1.0	1.2
Ramachandran plot, % non-glycine or non-proline residues in								
Most favored regions	88.1	85.1	88.0	84.3	82.3	85.1	93.2	88.8
Additional allowed regions	11.9	13.7	10.8	14.1	15.7	12.5	6.8	10.8
Generously allowed region	0.0	1.2	1.2	1.6	2.0	2.4	0.0	0.4
Disallowed regions	0.0	0.0	0.0	0.0	0.0	0.0	0.0	0.0
Expected coordinate error from Luzzati plot (Å)	0.34	0.30	0.31	0.35	0.38	0.45	0.30	0.38

collected from oxyhaemoglobin crystals at r.h. values of 98 and 95% and from deoxyhaemoglobin crystals at r.h. values of 95 and 93%, as the unit-cell parameters at these r.h. values were nearly the same as those of the respective native crystals. Crystal data, data-collection statistics and refinement statistics pertaining to the data collected and used in the analysis are given in Table 1.

3.2. Haem stereochemistry

The tertiary structure of the protein is remarkably similar in all the crystal forms. However, the position of the ferrous iron with respect to the porphyrin ring in the low-humidity deoxy crystal presents an interesting case. The relevant distances in the native high-salt (Fermi *et al.*, 1984) and low-salt (Kavanaugh *et al.*, 1992) deoxy crystals, in the native oxy crystals and in the two molecules of the 90% r.h. form are listed in Table 2 and illustrated in Fig. 4. As is well known, the ferrous iron shifts from the haem plane towards the proximal histidine by about 0.6 Å (by about 0.4 Å from the plane of the porphyrin N atoms) in the deoxy form, while it lies in the plane in the oxy form in both the subunits. Consequently, the distance between the ferrous iron and the coordinating N atoms are a little longer in the former. Surprisingly, the displacement of the ferrous iron from the haem plane and the Fe–N distances in

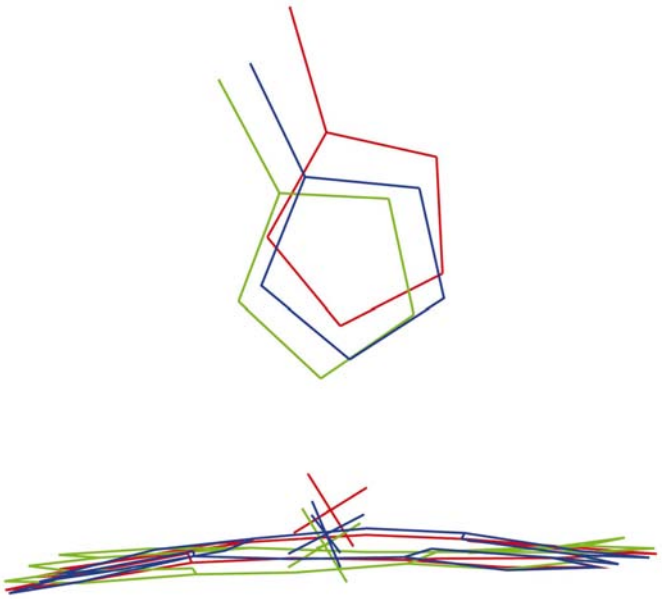

Figure 4
Haem environment of the α-subunit of native deoxy (red), molecule 1 of deoxy 90% r.h. (blue) and oxy (green) structures.

the low-humidity deoxy form are closer to those in the oxy form than to those in the native deoxy form. Thus, the removal of a small amount of water from the crystals of the deoxy form appears to have the effect of driving the haem stereochemistry towards that in the oxy form.

The above result was rather surprising and it was important to critically examine its reliability. Each of the distances quoted in Table 2 is an average over at least two observations except in the case of the native oxy structure. Of the distances, those between the mean plane of the porphyrin N atoms and the ferrous iron are expected to be quite reliable, as each such distance involves a mean plane calculated using four atoms and a comparatively heavy and hence better defined metal ion. The distance between the ferrous ion and porphyrin N atoms is also expected to be reliable as the value is averaged over at least four and most often eight observations. The remaining two distances involve at one end a metal ion or a mean plane, but a single atom at the other end. The relevant distances in oxyhaemoglobin have similar values in all oxy structures refined by us and in the structure obtained by Shaanan (1983). The same is true in relation to the native deoxy structure refined by us and that obtained by Fermi *et al.* (1984). These similarities indicate that the results are not artifacts of refinement.

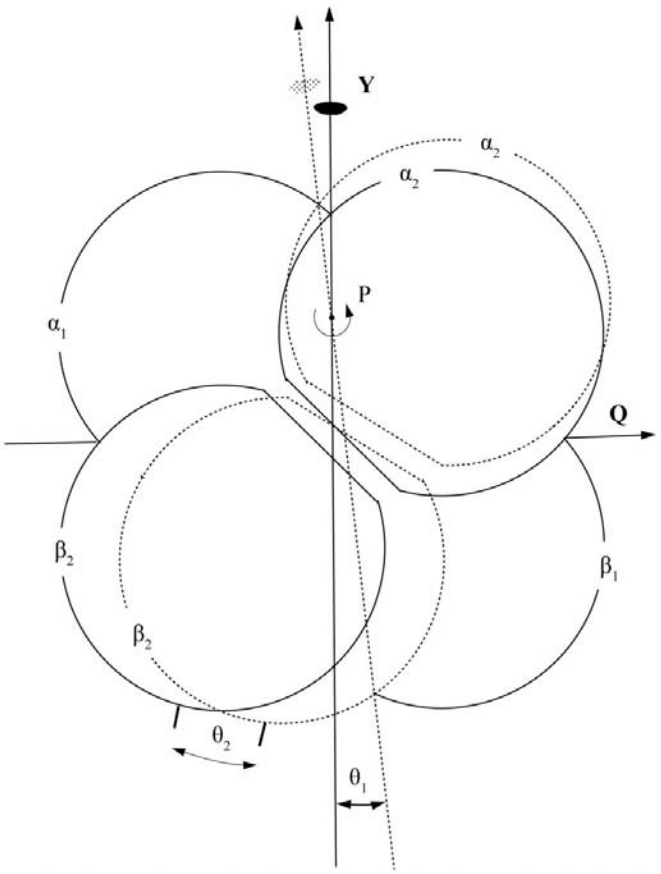

Figure 5
Schematic diagram showing the movement of $\alpha_2\beta_2$ relative to $\alpha_1\beta_1$ on going from unliganded (thick line) to liganded (dotted line) states. The movement also involves a small translation along P. The figure has been adapted from Fig. 7 in Baldwin & Chothia (1979).

Table 2
Haem stereochemistry.

Distances are in Å.

	1†	2‡	3§	4¶
Deoxy				
α	0.45	2.1	2.0	2.5
β	0.33	2.1	2.2	2.5
Deoxy (low salt)				
α	0.41	2.1	2.0	2.6
β	0.36	2.1	2.1	2.5
Oxy				
α	0.12	2.0	1.9	2.0
β	0.11	2.0	2.1	2.0
Deoxy 90% r.h. molecule 1				
α	0.15	2.0	2.1	2.2
β	0.16	2.0	2.3	2.5
Deoxy 90% r.h. molecule 2				
α	0.17	2.0	2.1	2.3
β	0.13	2.0	2.3	2.4

† The perpendicular distance from the plane of the porphyrin N atoms to the ferrous ion. ‡ The average distance between the ferrous ion and the N atoms of the porphyrin. § The distance between the ferrous ion and the NE2 atom of the proximal histidine. ¶ The perpendicular distance from the plane of the porphyrin N atoms to the NE2 atom of the proximal histidine.

Table 3
R.m.s. deviations (Å) in the main-chain atoms resulting from the superposition of the $\alpha_1\beta_1$ subunits of pairs of molecules.

Values for the $\alpha_1\beta_1$ subunits are given in the lower left half of the table and those for the $\alpha_2\beta_2$ subunits in the upper right half.

	1†	2‡	3§	4¶	5††	6‡‡	7§§	8¶¶	9†††	10‡‡‡
1	—	0.65	0.61	0.82	0.72	0.78	5.08	5.54	4.95	5.72
2	0.38	—	0.30	0.60	0.58	0.82	5.02	5.48	4.89	5.66
3	0.34	0.22	—	0.61	0.56	0.76	5.00	5.47	4.88	5.64
4	0.46	0.32	0.31	—	0.49	0.68	5.08	5.49	4.94	5.66
5	0.38	0.28	0.30	0.32	—	0.48	5.07	5.53	4.97	5.72
6	0.46	0.22	0.44	0.54	0.38	—	4.98	5.42	4.86	5.62
7	0.75	0.64	0.62	0.72	0.73	0.81	—	0.86	0.56	0.83
8	0.75	0.63	0.63	0.68	0.71	0.79	0.43	—	1.04	0.49
9	0.70	0.62	0.57	0.67	0.67	0.77	0.48	0.45	—	1.12
10	0.75	0.62	0.61	0.69	0.68	0.80	0.22	0.35	0.50	—

† Oxy native. ‡ Oxy 93%. § Oxy 90%. ¶ Oxy 88%. †† Oxy 84%. ‡‡ Oxy 25% methanol. §§ Deoxy native. ¶¶ Deoxy 90% molecule 1. ††† Deoxy 90% molecule 2. ‡‡‡ Human deoxy low salt.

3.3. Quaternary structure

The molecules in the native crystals of oxyhaemoglobin, those at r.h. values of 93, 90, 88 and 84%, that partially dehydrated using 25% methanol, that of native deoxyhaemoglobin, its 90% r.h. form (two molecules) and that of deoxyhaemoglobin grown at low salt were considered for detailed comparisons. One $\alpha\beta$ dimer from one molecule was superposed on an $\alpha\beta$ dimer in the other molecule in each pair. The r.m.s. deviations in main-chain atoms in the superposed dimers ($\alpha_1\beta_1$ subunits) and those in the dimers which were not superposed ($\alpha_2\beta_2$ subunits), were calculated. These values are listed in Table 3. The first set of values involving oxyhaemoglobin molecules clearly show that there is no systematic variation in the internal structure of the $\alpha\beta$ dimer

as a function of solvent content. Independent superposition of α- and β-subunits also corroborated this conclusion.

The changes in the quaternary structure of haemoglobin associated with oxygen binding primarily involves the movement of one $\alpha\beta$ dimer as a whole with respect to the other. The r.m.s. deviation in main-chain atoms of the $\alpha_2\beta_2$ dimers obtained on the superposition of the $\alpha_1\beta_1$ dimers of a pair of molecules gives a rough and ready estimate of this movement (Silva *et al.*, 1992). Such deviations in every pair of molecules under consideration are listed in the upper right half of Table 3. As shown by Baldwin & Chothia (1979) and illustrated in Fig. 5, the movements can be described in terms of a screw rotation angle (θ_2 in Fig. 5), the screw rotation translation, the direction of the screw rotation axis and a point on the rotation axis. The same parameters can be used to describe the relationship between the quaternary structures of any two haemoglobin molecules. The values of all four parameters for pairs of different molecules are given in the lower left part of Fig. 6. The first line in the boxes in the lower left part of Fig. 6 corresponds to angle θ_2 and the translation (given in parentheses). The second line indicates the direction of the rotation axis, whereas the third line defines a point on the rotation axis. Also given is the angle θ_1 between the axes that relate $\alpha_1\beta_1$ and $\alpha_2\beta_2$ dimers. These calculations were performed using the computer program *ALIGN* (Cohen, 1997).

The information presented in Table 3 and Fig. 6 indicates no systematic change in quaternary association in the oxyhaemoglobin molecules as a function of water content. On the contrary, systematic though small changes are associated with the deoxyhaemoglobin molecules. Deoxyhaemoglobin molecules in all the crystal forms have, as a group, quaternary structures substantially different to those of oxyhaemoglobin molecules. This difference is characterized by r.m.s. deviations of around 5 Å in main-chain atoms in $\alpha_2\beta_2$ subunits when $\alpha_1\beta_1$ subunits are superposed and rotations of about 13° of the $\alpha_2\beta_2$ dimer with respect to the $\alpha_1\beta_1$ dimer. There are, however, small variations within deoxy molecules. For instance, the r.m.s. deviations and the angles clearly show that the quaternary structure of the deoxy molecule in the high-salt crystals is closer to that of the oxygenated molecules than that of the deoxy molecule in the low-salt crystals. It also turns out that the two crystallographically independent molecules that result when the high-salt form undergoes a water-mediated transformation at 90% r.h. have somewhat different quaternary structures. The quaternary association in one of them moves closer to that in the oxygenated molecule, while that of the other moves further away from the oxygenated form towards that in the low-salt crystals. The difference between the quaternary structures of the two molecules is quite substantial. The r.m.s. deviations in the main-chain atoms between $\alpha_2\beta_2$ subunits when the $\alpha_1\beta_1$ subunits in the molecules are superposed turn out to be more than 1 Å. The difference also involves a rotation of more than 2° of one of the $\alpha\beta$ dimers. The differences between the molecules in the high-salt and the low-salt crystals could well be considered to have arisen from differences in the composition of the medium. In the low-humidity form, the two crystallographically independent molecules exist in the same medium. Therefore, the two quaternary structures observed in this form

	1	2	3	4	5	6	7	8	9	10
1	–	0.2	0.2	0.8	0.6	0.5	6.5	6.8	6.3	7.2
2	0.4 (0.5) (17.9 90.0 72.1) (−15.3 10.2 3.5)	–	0.1	0.6	0.4	0.4	6.7	7.0	6.5	7.3
3	0.4 (0.4) (48.6 90.0 41.4) (−21.8 −15.0 6.6)	0.2 (−0.1) (74.7 90.0 25.3) (−0.9 −17.2 3.4)	–	0.6	0.5	0.4	6.7	7.0	6.5	7.4
4	1.5 (0.1) (13.8 90.0 76.2) (−14.8 18.2 −4.0)	1.2 (−0.3) (23.2 90.0 76.8) (−16.1 6.8 −5.7)	1.3 (−0.2) (29.7 90.0 60.3) (−17.6 5.3 −6.7)	–	0.2	0.2	7.0	7.3	6.8	7.7
5	1.2 (0.2) (9.8 90.0 80.2) (−14.1 19.2 1.4)	0.8 (−0.3) (7.7 90.0 82.3) (−13.9 18.1 0.9)	1.0 (−0.3) (6.3 90.0 83.7) (−14.0 11.3 −2.2)	0.5 (−0.0) (73.3 90.0 16.7) (−1.0 −10.0 3.4)	–	0.0	7.1	7.5	6.9	7.9
6	1.0 (−0.1) (1.4 90.0 88.6) (−13.9 24.5 −1.1)	0.8 (−0.5) (9.1 90.0 80.8) (−14.1 12.5 −2.9)	0.8 (−0.5) (20.7 90.0 69.3) (−15.6 2.9 −5.4)	0.4 (−0.2) (51.7 90.0 38.3) (−5.1 −28.2 6.5)	0.1 (0.0) (69.1 90.0 20.9) (−1.8 41.5 −4.9)	–	7.0	7.3	6.8	7.7
7	13.0 (1.6) (29.4 90.0 60.6) (−12.2 11.6 −6.2)	13.4 (1.0) (28.6 90.0 61.4) (12.5 11.4 −6.3)	13.4 (1.1) (29.6 90.0 60.4) (−12.5 10.5 −6.6)	14.0 (0.9) (24.6 90.0 65.4) (−12.9 9.8 −5.6)	14.2 (1.1) (27.6 90.0 62.4) (−12.5 8.9 −6.1)	14.0 (1.2) (26.4 90.0 63.6) (−12.6 8.5 −5.9)	–	0.8	0.5	0.9
8	13.6 (2.1) (34.6 90.0 55.4) (−9.9 11.4 −7.4)	14.0 (1.4) (34.2 90.0 65.8) (−10.1 11.3 −7.4)	14.0 (1.5) (35.1 90.0 54.9) (−10.1 10.7 −7.4)	14.6 (1.3) (30.0 90.0 60.0) (−11.1 9.9 −6.7)	15.0 (1.5) (32.8 90.0 57.2) (−10.6 9.0 −7.3)	14.6 (1.6) (31.8 90.0 58.2) (−10.7 8.6 −7.1)	1.6 (0.2) (74.8 90.0 15.2) (3.2 −1.8 −3.6)	–	1.1	0.4
9	12.5 (1.6) (27.7 90.0 72.3) (−12.1 11.4 −6.1)	13.0 (1.1) (27.6 90.0 62.4) (−12.1 11.0 −6.1)	13.0 (1.2) (28.3 90.0 61.7) (−12.1 10.6 −6.1)	13.6 (1.1) (23.2 90.0 66.8) (−12.9 9.4 −5.3)	13.8 (1.2) (26.4 90.0 63.6) (−12.4 8.7 −6.0)	13.6 (1.3) (25.5 90.0 64.5) (−12.5 7.9 −5.6)	1.0 (0.1) (8.0 90.0 82.0) (−11.4 11.8 13.8)	2.2 (−0.1) (64.8 90.0 25.2) (9.3 −1.8 11.1)	–	1.1
10	14.4 (2.1) (34.0 90.0 56.0) (−10.6 11.3 −7.5)	14.6 (1.4) (33.3 90.0 56.7) (−10.8 11.2 −7.5)	14.8 (1.4) (34.2 90.0 55.8) (−10.4 10.4 −7.8)	15.4 (1.3) (29.4 90.0 60.6) (−11.4 9.8 −6.7)	15.8 (1.5) (32.4 90.0 57.6) (−11.1 8.8 −7.4)	15.4 (1.6) (31.4 90.0 58.6) (−11.1 8.6 −7.2)	1.8 (0.3) (67.0 90.0 23.0) (2.1 3.4 −6.9)	0.8 (0.0) (52.9 90.0 37.1) (−11.9 2.0 −8.3)	2.2 (0.4) (65.2 90.0 34.8) (1.0 10.6 −7.9)	–

Figure 6
Angles (°) θ_1 (upper right) and θ_2 (lower left) that define the relation between pairs of tetramers (Fig. 5). The translation, direction of rotation axis and a point on rotation axis are also given in the lower left of the figure. The numbering of structures is the same as in Table 3. See text for details.

are likely to correspond to two states naturally accessible to deoxyhaemoglobin.

4. Conclusions

Contrary to expectations, changes in the environmental humidity or solvent content of the crystals did not lead to any change in the structure of oxyhaemoglobin. Surprisingly, on the other hand, the haem geometry in deoxyhaemoglobin at low environmental humidity and slightly low solvent content mimics that in oxyhaemoglobin. The molecules in the native low-salt and high-salt deoxyhaemoglobin crystals and the two crystallographically independent molecules in the low-humidity form present an ensemble of slightly different quaternary structures representing the T state.

The authors thank R. K. Rath for help with the preparation of samples. The data were collected using the National Facility for Structural Biology supported by the Departments of Science and Technology (DST) and Biotechnology (DBT). Facilities at the Supercomputer Education and Research Centre of the Institute and the Bioinformatics Centre and the Graphics Facility supported by the DBT were used for computations. The work is supported by the Council of Scientific and Industrial Research.

References

Baldwin, J. & Chothia, C. (1979). *J. Mol. Biol.* **129**, 175–220.
Biswal, B. K., Sukumar, N. & Vijayan, M. (2000). *Acta Cryst.* D**56**, 1110–1119.
Biswal, B. K. & Vijayan, M. (2001). *Curr. Sci.* **81**, 1100–1105.
Bolton, W. & Perutz, M. F. (1970). *Nature (London)*, **228**, 551–552.
Boyes-Watson, J., Davidson, E. & Perutz, M. F. (1947). *Proc. R. Soc. London Ser. A*, **191**, 83–132.
Brünger, A. T., Adams, P. D., Clore, G. M., Delano, W. L., Gros, P., Grosse-Kunstleve, R. W., Jiang, J.-S., Kuszewski, J., Nilges, M., Pannu, N. S., Read, R. J., Rice, L. M., Simonson, T. & Warren, G. L. (1998). *Acta Cryst.* D**54**, 905–921.
Cohen, G. E. (1997). *J. Appl. Cryst.* **30**, 1160–1161.
Colombo, M. F., Rau, D. C. & Parsegian, V. A. (1992). *Science*, **256**, 655–659.
Colombo, M. F. & Seixas, F. A. C. (1999). *Biochemistry*, **38**, 11741–11748.
Fermi, G., Perutz, M. F. & Shaanan, B. (1984). *J. Mol. Biol.* **175**, 159–174.
Huxley, H. E. & Kendrew, J. C. (1953). *Acta Cryst.* **6**, 76–80.
Jones, T. A. (1978). *J. Appl. Cryst.* **11**, 268–272.
Kavanaugh, J. S., Rogers, P. H., Case, D. A. & Arnone, A. (1992). *Biochemistry*, **31**, 4111–4121.
Kodandapani, R., Suresh, C. G. & Vijayan, M. (1990). *J. Biol. Chem.* **265**, 16126–16131.
Kroeger, K. E. & Kundrot, C. E. (1997). *Structure*, **5**, 227–237.
Kuriyan, J., Wilz, S., Karplus, M. & Petsko, G. A. (1986). *J. Mol. Biol.* **192**, 133–154.
Laskowski, R. A., MacArthur, M. W., Moss, D. S. & Thornton, J. M. (1993). *J. Appl. Cryst.* **26**, 283–291.
Madhusudan & Vijayan, M. (1991). *Curr. Sci.* **60**, 165–170.
Madhusudan, Kodandapani, R. & Vijayan, M. (1993). *Acta Cryst.* D**49**, 234–245.
Matthews, B. W. (1968). *J. Mol. Biol.* **33**, 491–497.
Monod, J., Wyman, J. & Changeux, J. P. (1965). *J. Mol. Biol.* **12**, 88–118.
Mueser, T. C., Rogers, P. H & Arnone, A. (2000). *Biochemistry*, **39**, 15353–15364.
Nagendra, H. G., Sudarsanakumar, C. & Vijayan, M. (1995). *Acta Cryst.* D**51**, 390–392.
Nagendra, H. G., Sudarsanakumar, C. & Vijayan, M. (1996). *Acta Cryst.* D**52**, 1067–1074.
Nagendra, H. G., Sukumar, N. & Vijayan, M. (1998). *Proteins Struct. Funct. Genet.* **32**, 229–240.
Navaza, J. (1994). *Acta Cryst.* A**50**, 157–163.
Otwinowski, Z. & Minor, W. (1997). *Methods Enzymol.* **276**, 307–325.
Perutz, M. F. (1954). *Proc. R. Soc. London Ser. A*, **225**, 264–286.
Perutz, M. F. (1968). *J. Cryst. Growth*, **2**, 54–56.
Perutz, M. F. (1970). *Nature (London)*, **228**, 726–734.
Perutz, M. F., Muirhead, H., Cox, J. M. & Goaman, L. C. G. (1968). *Nature (London)*, **219**, 131–139.
Perutz, M. F., Wilkinson, A. J., Paoli, M. & Dodson, G. G. (1998). *Annu. Rev. Biophys. Biomol. Struct.* **27**, 1–34.
Radha Kishan, K. V., Chandra, N. R., Sudarsanakumar, C., Suguna, K. & Vijayan, M. (1995). *Acta Cryst.* D**51**, 703–710.
Sadasivan, C., Nagendra, H. G. & Vijayan, M. (1998). *Acta Cryst.* D**54**, 1343–1352.
Salunke, D. M., Veerapandian, B., Kodandapani, R. & Vijayan, M. (1985). *Acta Cryst.* B**41**, 431–436.
Salunke, D. M., Veerapandian, B. & Vijayan, M. (1984). *Curr. Sci.* **53**, 231–235.
Shaanan, B. (1983). *J. Mol. Biol.* **171**, 31–59.
Silva, M. M., Rogers, P. H. & Arnone, A. (1992). *J. Biol. Chem.* **267**, 17248–17256.
Smith, F. R. & Simmons, K. C. (1994). *Proteins Struct. Funct. Genet.* **18**, 295–300.
Sukumar, N., Biswal, B. K. & Vijayan, M. (1999). *Acta Cryst.* D**55**, 934–937.
Tame, J. R. H. (1999). *Trends Biochem. Sci.* **24**, 372–377.
Vijayan, M. (1980). *Computing in Crystallography*, edited by R. Diamond, S. Ramaseshan & K. Venkateshan, pp 19.01–19.26. Bangalore: Indian Academy of Sciences.